Study on Free Vibration of Plates with Variable Thickness and a Hole Defect

by
X.Q Ma*, C. Morita ** , T. Sakiyama***, H. Matsuda***, M. Huang ***

The objective of this paper is to clarify the characteristics of vibration of plates with variable thickness and a hole defect by analytical and experimental methods. The vibration frequencies and modes obtained by the proposed discrete method are verified with the experimental results. Moreover, the effects of the thickness of plates, size of the defect on free vibration behavior of plates are also investigated.

***Key word**: free vibration, discrete method, Green function, a hole defect, variable thickness*

1. INTRODUCTION

Plates with variable thickness are frequently used in order to economize on the plate materials or to lighten the plates, especially when used in wings for high-speed, high-performance aircrafts. By carefully designing the thickness distribution, a substantial increase in stiffness, buckling and vibration capacities of the plate may be obtained over its uniform thickness counterpart. Many researchers [1-7] have analyzed the free vibration of plates with variable thickness for many years. In this paper, a discrete method is proposed to analyze the bending and free vibration problems of plates. No prior assumption of shape of deflection, such as shape function used in Rayleigh-Ritz method, is employed in the proposed method. The fundamental differential equations involving Dirac's delta functions are established and satisfied exactly throughout the whole plate. By transforming these equations into the integral equations and using numerical integration, the solutions are obtained at the discrete points. The solutions are only related to the unknown quantities along the boundary. That makes the number of the unknown quantities decrease greatly. The Green function, which is the solution for deflection, is used to obtain the characteristic equation of the free vibration. The convergence and accuracy of the numerical results are compared with experimental results. Moreover, the effects of the thickness of plates, size of the defect on free vibration behavior of plates are shown.

2. A DISCRETE METHOD

2.1 Discrete green function

In order to obtain the fundamental differential equation of a rectangular plate with variable thickness, an *x-y-z* coordinate system is used with its *x-y* plane contained in middle plane of a rectangular plate and the *z*-axis perpendicular to the middle plane of the plate. The thickness, the length and the width of the rectangular plate are *h, a* and *b*, respectively. The principle material axes of the plate in the longitudinal, transverse and normal directions are designated as 1, 2 and 3 (shown in Ref.[8]).

In this paper, the distributed load $\overline{q} = \overline{q}(x, y)$ is considered for the analysis of the rectangular cantilever plate.

The fundamental differential equations of plates with variable thickness are as follows.

$$\frac{\partial Q_x}{\partial x} + \frac{\partial Q_y}{\partial y} + \overline{q} = 0 , \qquad \frac{\partial M_{xy}}{\partial x} + \frac{\partial M_y}{\partial y} - Q_y = 0 ,$$

$$\frac{\partial M_x}{\partial x} + \frac{\partial M_{xy}}{\partial y} - Q_x = 0 , \quad \frac{\partial \theta_x}{\partial x} + \nu \frac{\partial \theta_y}{\partial y} = \frac{M_x}{D} ,$$

Received on Nov. 30, 2007

* Foreign Visiting Scholar of Department of Structural Engineering
** Graduate School of Science and Technology
*** Department of Structural Engineering

$$\frac{\partial\theta_y}{\partial y}+\nu\frac{\partial\theta_x}{\partial x}=\frac{M_y}{D},\qquad \frac{\partial\theta_x}{\partial y}+\frac{\partial\theta_y}{\partial x}=\frac{2}{(1-\nu)}\frac{M_{xy}}{D},$$
$$\frac{\partial w}{\partial x}+\theta_x=\frac{Q_x}{Gt_s},\qquad \frac{\partial w}{\partial y}+\theta_y=\frac{Q_y}{Gt_s} \tag{1}$$

where Q_x and Q_y are the shearing forces, M_{xy} *(= M_{yx})* is the twisting moment, M_x and M_y are the bending moments, θ_x and θ_y are rotations of the normal to the middle plane in the *y*- and *x*-directions, *w* is the deflection, $D = Eh^3/12(1-\nu^2)$ is the flexural rigidity of the plate, *E* is the modulus of elasticity, *G* is the shear modulus of elasticity, ν is the Possion`s ratio, *h=h(x, y)* is the thickness of the plate, $t_s=h/1.2$, $\bar{q}=\bar{q}(x,y)$ is the distributed load. The following non-dimensional expressions are introduced in the proposed discrete method.

$$\begin{bmatrix}X_1 & X_2\end{bmatrix}=\frac{a^2}{D_0(1-\nu^2)}\begin{bmatrix}Q_y & Q_x\end{bmatrix}$$

$$\begin{bmatrix}X_3 & X_4 & X_5\end{bmatrix}=\frac{a}{D_0(1-\nu^2)}\begin{bmatrix}M_{xy} & M_y & M_x\end{bmatrix},$$

$$\begin{bmatrix}X_6 & X_7 & X_8\end{bmatrix}=\begin{bmatrix}\theta_y & \theta_x & \frac{w}{a}\end{bmatrix},\quad \begin{bmatrix}\eta & \zeta\end{bmatrix}=\begin{bmatrix}\frac{x}{a} & \frac{y}{b}\end{bmatrix}$$

By transforming equation (1) into the integral equation and applying the trapezoidal rule of the approximate numerical integration, the discrete solution of equation (1) at point *(i, j)* (shown in Fig. 1) is obtained as

$$X_{pij}=\sum_{d=1}^{6}\left\{\sum_{f=0}^{i}a_{pijfd}X_{rfo}+\sum_{g=0}^{j}b_{pijgd}X_{sog}\right\}+\bar{q}_{pij}P \tag{2}$$

Where a_{pijfd}, b_{pijgd}, $\bar{q}_{pij}$ are given in Ref.[8].

From equation (2), it can be found that the quantity X_{pij} at the discrete point *(i, j)* is only related to the quantities X_{rf0} *(r=1,3,4,6,7,8)* and X_{s0g} *(r=2,3,5,6,7,8)* at the boundary dependent points.

By applying the Green function $w(x_0,y_0,x,y)/\bar{P}$, which is the displacement of point (x_0,y_0) of a plate with a unite concentrated load at point (x,y), the displacement amplitude $\hat{w}(x_0,y_0)$ of point (x_0,y_0) of the plate during free vibration is given as follows:

$$\hat{w}(x_0,y_0)=\int_0^b\int_0^a\rho h\omega^2\hat{w}(x,y)[w(x_0,y_0,x,y)/\bar{P}]dxdy \tag{3}$$

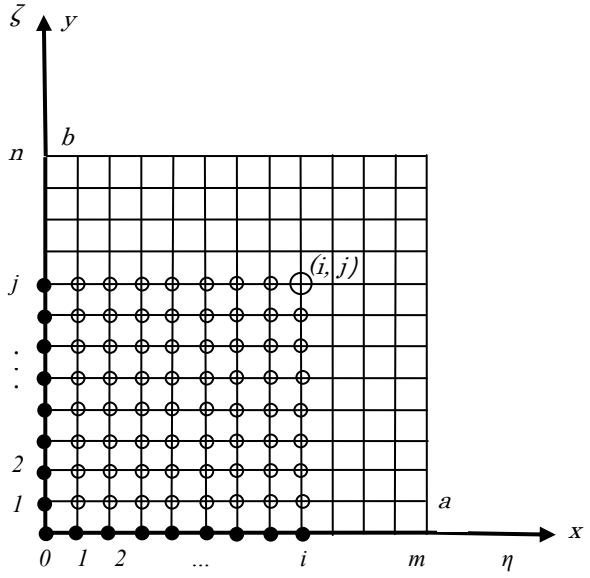

Fig.1 Discrete points on a plate

By using the numerical integration method and the following non-dimensional expressions,

$$\lambda^4=\frac{\rho_0h_0\omega^2a^4}{D_0(1-\nu^2)},\qquad \Lambda=\frac{1}{\mu\lambda^4},$$
$$H(\eta,\zeta)=\frac{\rho(x,y)}{\rho_0}\frac{h(x,y)}{h_0},\quad W(\eta,\zeta)=\frac{\hat{w}(x,y)}{a},$$
$$G(\eta_0,\zeta_0,\eta,\zeta)=\frac{w(x_0,y_0,x,y)}{a}\frac{D_0(1-\nu^2)}{\bar{P}a}$$

where ρ_0 is the standard mass density and ω is the circular frequency, the characteristic equation is obtained from equation (3) as

$$\sum_{i=0}^{m}\sum_{j=0}^{n}(\beta_{mi}\beta_{nj}H_{ij}G_{klij}-\Lambda\delta_{ik}\delta_{jl})W_{ij}=0 \tag{4}$$

where $\delta_{ik}=\begin{cases}0; & if\ i\neq k\\ 1; & if\ i=k\end{cases}$, $\delta_{jl}=\begin{cases}0; & if\ j\neq l\\ 1; & if\ j=l\end{cases}$

2.2 Equivalent rectangular plate with a hole defect

A plate with a hole defect can be transformed into an equivalent plate with non-uniform thickness (shown in Fig. 2) by considering the hole as a thin part of the plate theoretically. The thickness of the actual part of original plate is expressed as *h*, and the thickness of the thin part of the equivalent plate is expressed as h_t. The thickness of the plate along the border line between the actual part and the thin part is chosen as $(h+h_t)/2$.

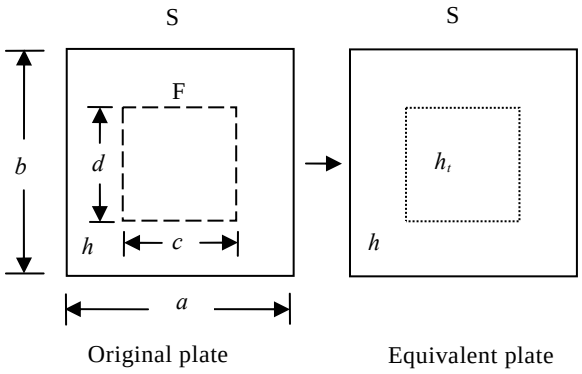

Fig.2 A plate with a hole defect and its equivalent plate

3. HOLOGRAPHIC INTERFEROMETRY

In the experimental study, the specimen on which the strain gauges are affixed, are fixed in the fixture and acoustically excited by a siren. Oscillation frequencies at the maximum output of strain gauges are considered as resonance frequencies. These resonance vibration modes are obtained by forming a hologram on photographic plate, using the time-average method of holographic interferometry. The experimental device and principle of hologram [9] are shown in Fig. 3 and Fig. 4, respectively.

4. EXPERIMENTAL AND ANALYTICAL RESULTS

In this experiment, aluminum alloy plates are used as specimen and the dimensions and material properties are given in Table 1.

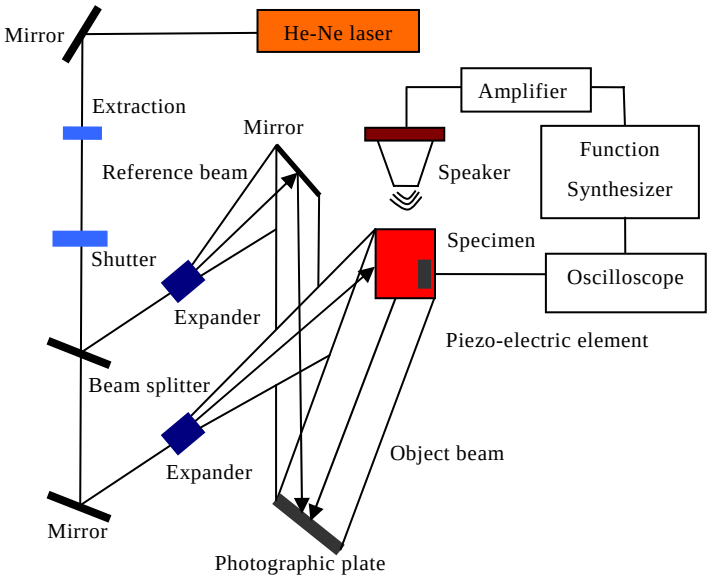

Fig.3 Laser holography instrument

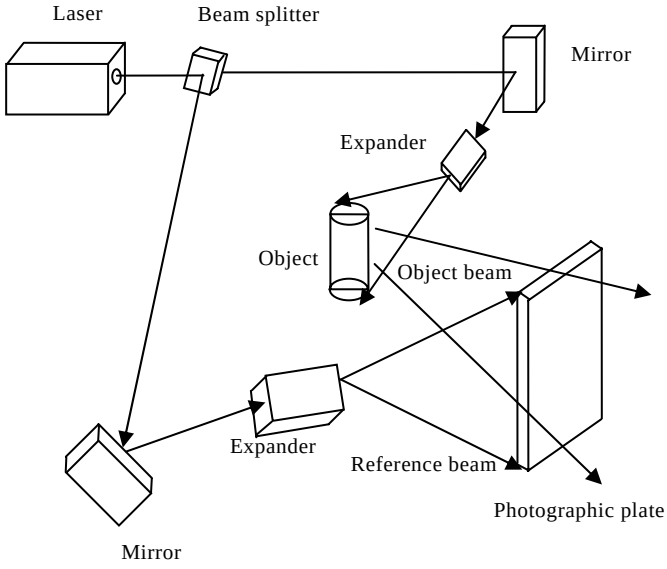

Fig.4 Principle of hologram

4.1 Plates with uniform thickness

Firstly, in order to investigate the convergence and accuracy of the analytical results, the isotropic uniform cantilever plates are used to obtain frequencies and vibration modes by laser holographic interferometry. For the aluminum alloy cantilever plates, the convergence and accuracy of the lowest six modes frequencies with number of divisions and the extrapolated values are shown in Table2, together with the analytical results obtained by Ref.[1] and experimental results. Fig.5 shows the lowest six nodal patterns of experimental and analytical results.

Table1 Properties of the specimen of aluminum alloy

$a \times b \times h$ (mm)	E (GPa)	G (GPa)	ν	ρ (KN/m^3)
90×90×1	69.6	26.1	0.33	26.5

Table2 Convergence and accuracy of frequencies

$m=n$	1st	2nd	3rd	4th	5th	6th
8	105.8	257.0	679.4	868.2	979.3	1738
12	105.5	255.2	658.0	842.6	949.7	1674
Ex.v, 8-12	105.3	253.7	640.9	822.1	926.1	1622
Ref.[1]	105.7	260.3	648.3	828.2	947.0	1653
Experiment	100.0	245.0	580.0	815.0	890.0	1520

Ex.: The values obtained by using Richardson`s extrapolation formula

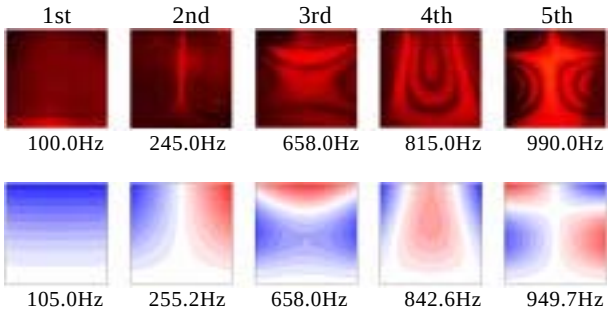

Fig.5 Nodal patterns for plates with uniform thickness (Upper: experimental; lower: analytical)

4.2 Plates with non-uniform thickness

Four types of plates with non-uniform thickness are used in the experiment, plate shapes refer to Fig.6. Nodal patterns are shown in Fig.7-Fig.10 (the left is for analytical results and the right is for experimental results). Holes in the Fig. 6 are used to fix the specimen in the experiments.

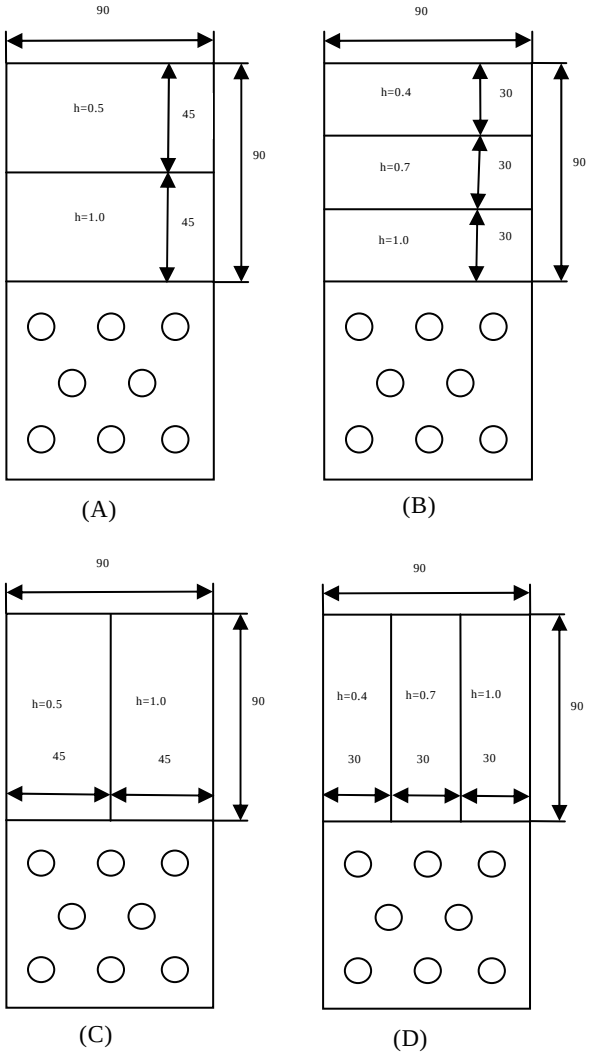

Fig.6 Four types of Specimen A, B, C and D of plates with non-uniform thickness (unit: mm)

For plates A and B (Fig. 7 and Fig. 8), the nodal patterns of 1st to 4th modes of analytical results are almost the same as experimental results. All of nodal lines are symmetrical to the vertical axis.

For plates C and D (Fig.9 and 10), because of plates with unsymmetrical thickness, nodal lines of 1st to 5th modes are not symmetrical to the vertical axis. Inclined nodal lines are obtained both in analytical and in experimental results. The experimental results are in agreement with analytical results.

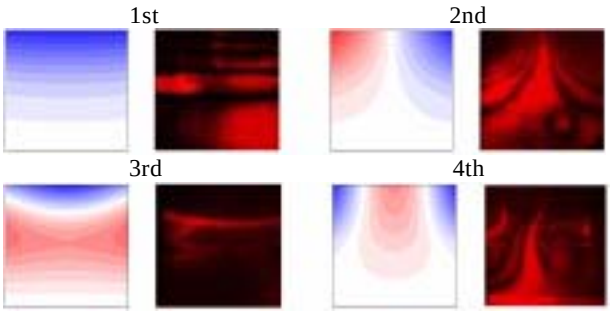

Fig.7 Comparison of nodal patterns of plate A

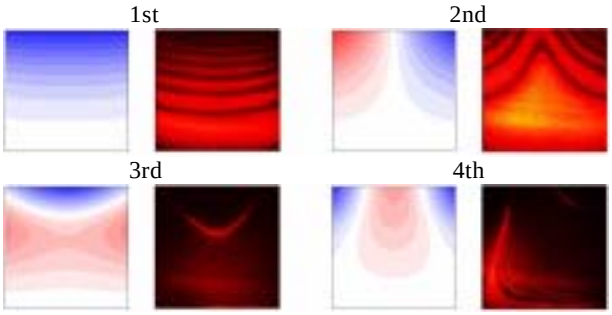

Fig.8 Comparison of nodal patterns of plate B

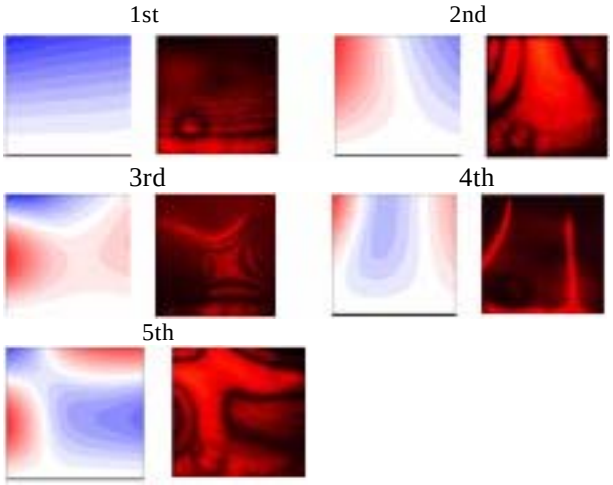

Fig.9 Comparison of nodal patterns of plate C

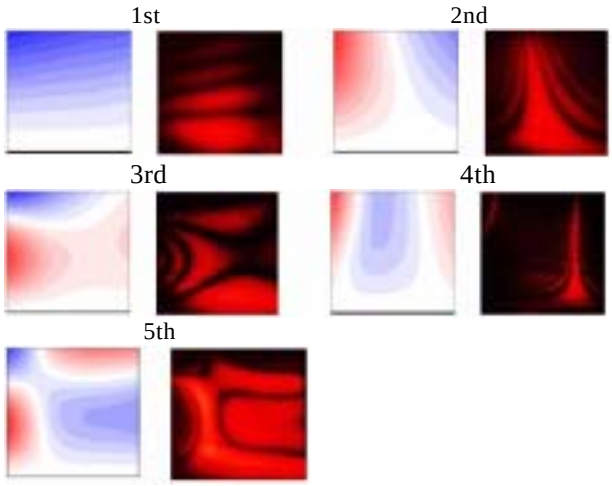

Fig.10 Comparison of nodal patterns of plate D

4.3 Plates with a hole defect

In this experiment, two types of hole defect are investigated for free vibration (Fig.11). The defect is located in the center of the plate. Nodal patterns are shown in Figs. 12 and 13 for analytical and experimental results of hole defect A and B. From 1st to 5th modes, the nodal patterns are the same as the uniform plate. So the nodal patterns from 1st to 5th mode are not shown.

Fig.14 shows the vibration frequencies of analytical and experimental results of defect A. From the experimental results, it is shown that the vibration frequencies of plate with a hole defect are in agreement with the analytical results. Compared with plate with defect B, the frequencies of plate with defect A are higher than of plate with defect B.

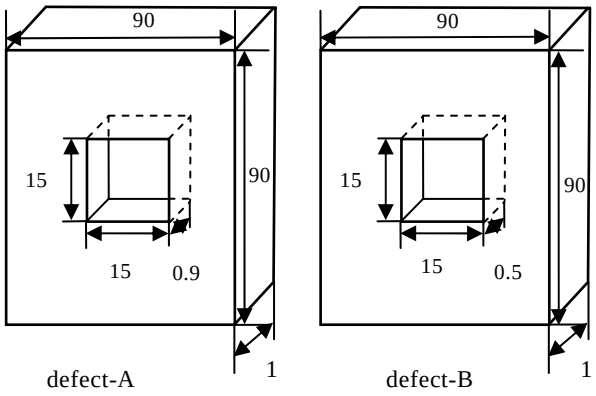

Fig.11 Plates with a hole defect (unit: mm)

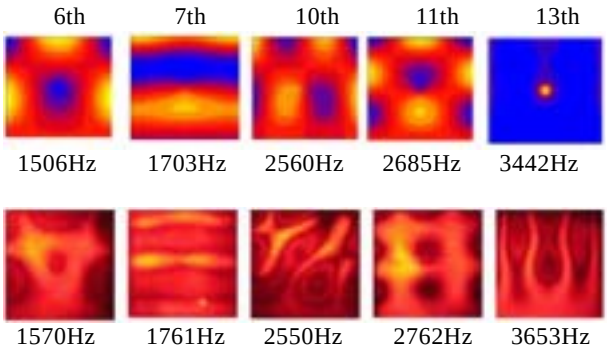

Fig.12 Comparison of nodal patterns of defect-A
(Upper: analytical; lower: experimental)

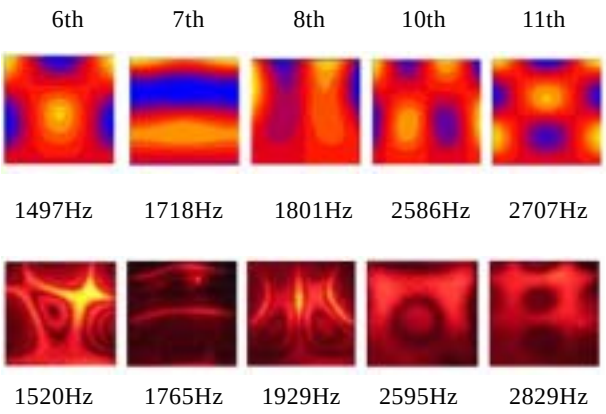

Fig.13 Comparison of nodal patterns of defect- B
(Upper: analytical; lower: experimental)

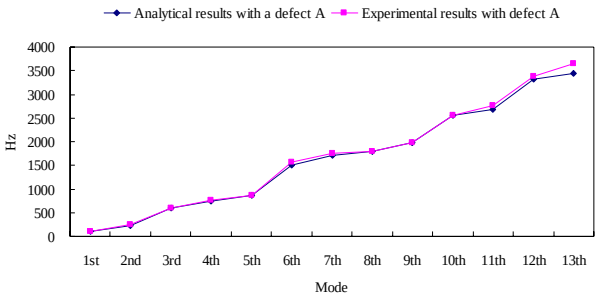

Fig.14 Vibration frequencies of analytical and experimental results (defect-A)

4.4 The effect of thickness of hole defect on vibration mode

Fig.15 shows the effect of thickness of hole defect on vibration mode. The size of all defects is chosen as 15mm ×15mm.

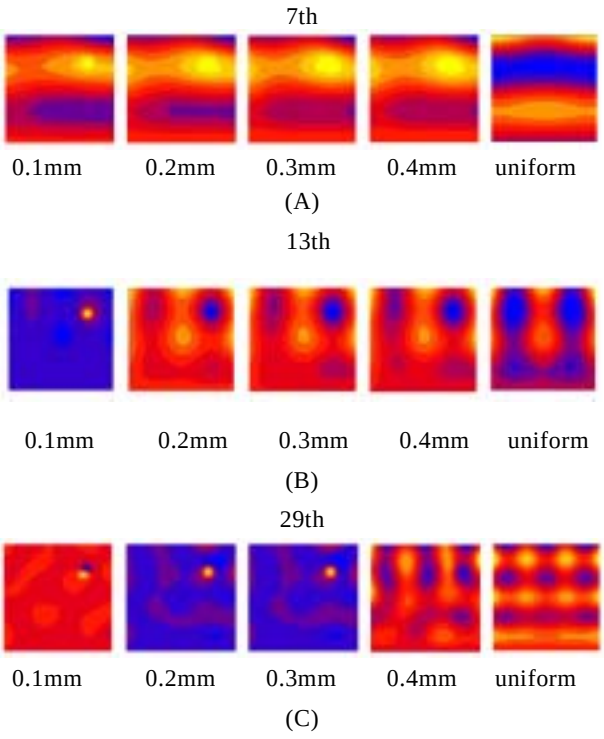

Fig.15 The effect of thickness of hole defect on vibration (Size of defect: 15mm×15mm)

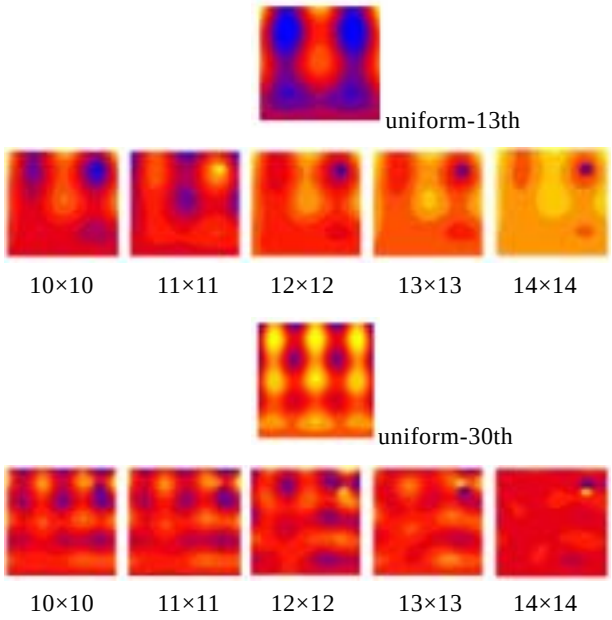

Fig. 16 The effect of size of hole defect on vibration (Thickness of defect: 0.1, unit: mm)

For 7th and 13th modes of plates with the thickness of defect of 0.1mm (Fig.15 A and B), it is shown that defect part will independently vibrate. If the thickness of defect is more than 0.2mm, there are changes happened compared with uniform plate and the defect can be detected out. But from 29th mode (Fig.15 C), there are 2 times resonance happened with thickness of defect with 0.1mm and the defect can be detected from the thickness of defect with 0.3mm.

4.5 The effect of size of defect on vibration mode

Fig.16 shows the effect of size of defect on vibration mode. The thickness of all hole defects is chosen as 0.1mm.

From 13th mode, the hole defect can be detected, when the size of defect is more than 11mm×11mm. From 30th mode, the hole defect can be detected, when the size of defect is more than 9mm×9mm. It is also shown that there are 2 times of resonance happened with size of defect 14mm×14mm, 13mm×13mm.

5. CONCLUSIONS

The objective of this paper is to clarify the characteristics of vibration of plates with variable thickness and a hole defect by analytical and experimental methods. It shows that the proposed results have a good convergence and satisfactory accuracy compared with experimental results. The effects of the thickness of plates, size of the defect on free vibration behavior of plates also investigated.

ACKNOWLEDGEMENT

The authors would like to thank Ms. Ayako Kanayama, Daiwa House Industry Co., Ltd.

REFERENCE

1) Classen RW and Thorne CJ. Vibration of a rectangular cantilever plates. *Journal of Aerospace Science* 1962; 29 (11): 1300-1305
2) H.T. Saliba, 1984, *Journal of Sound and Vibration*, 94, 381–395, Free vibration analysis of rectangular cantilever plates with symmetrically distributed point supports along the edges.
3) R.K. Roy, N. Ganesan, 1995, *Journal of Sound and Vibration,* 182, 355–367, Studies on the dynamic behavior of a square plate with varying thickness.
4) P. B. Bhat, P. A. A. Laura, R. G. Gutierrez, V. H. Cortinez, H. C. Sanzi, 1990, *Journal of Sound and*

Vibration, 138, 205–219, Numerical experiments on the determination of natural frequencies of transverse vibrations of rectangular plates of non-uniform thickness.

5) A. KAUSHAL and R. B. BHAT, *14th Canadian Congress of Applied Mechanics CANCAM`93*, A comparative study of vibration of plates with cutouts using the finite element and the Rayleigh Ritz methods.

6) K. M. Liew, T. Y. Ng, S. Kitipornchai, 2001, *Int. J. Solids Structures*, 38, 4937–4954. A semi-analytical solution for vibration of rectangular plates with abrupt thickness variation.

7) K. M. Liew, K. Y. Lam, S. T. Chow, 1990, *Computers and Structures* 34, 79–85, Free vibration analysis of rectangular plates using orthogonal plate function.

8) T. Sakiyama and M. Huang, 1998, *Journal and sound vibration,* 216, 379-397, Free vibration analysis of rectangular plates with variable thickness.

9) T. Kubouda, Holography Instruction, *Asakura Bookstore*, 1995